

RESEARCH ARTICLE

Wetland hydroperiod classification in the western prairies using multitemporal synthetic aperture radar

Joshua S. Montgomery^{1,3}  | Chris Hopkinson¹ | Brian Brisco² | Shane Patterson³ | Stewart B. Rood⁴ 

¹Department of Geography, University of Lethbridge, 4401 University Drive, Lethbridge, Alberta T1K3M4, Canada

²Canada Centre for Mapping and Earth Observation, 588 Booth St., Ottawa, Ontario K1A 0Y7, Canada

³Alberta Environment and Parks, 9920 108 Street, Edmonton, Alberta T5K 2M4, Canada

⁴Department of Environmental Science, University of Lethbridge, 4401 University Drive, Lethbridge, Alberta T1K3M4, Canada

Correspondence

Joshua S. Montgomery, Department of Geography, University of Lethbridge, 4401 University Drive, Lethbridge, Alberta T1K3M4, Canada.

Email: joshua.montgomery@uleth.ca

Funding information

Discovery Grant funding from the Natural Sciences and Engineering Research Council; Campus Alberta Innovates Program; Canada Foundation for Innovation

Abstract

Wetlands represent one of the world's most biodiverse and threatened ecosystem types and were diminished globally by about two-thirds in the 20th century. There is continuing decline in wetland quantity and function due to infilling and other human activities. In addition, with climate change, warmer temperatures and changes in precipitation and evapotranspiration are reducing wetland surface and groundwater supplies, further altering wetland hydrology and vegetation. There is a need to automate inventory and monitoring of wetlands, and as a study system, we investigated the Shepard Slough wetlands complex, which includes numerous wetlands in urban, suburban, and agricultural zones in the prairie pothole region of southern Alberta, Canada. Here, wetlands are generally confined to depressions in the undulating terrain, challenging wetlands inventory and monitoring. This study applied threshold and frequency analysis routines for high-resolution, single-polarization (HH) RADARSAT-2, synthetic aperture radar mapping. This enabled a growing season surface water extent hydroperiod-based wetland classification, which can support water and wetland resource monitoring. This 3-year study demonstrated synthetic aperture radar-derived multitemporal open-water masks provided an effective index of wetland permanence class, with overall accuracies of 89% to 95% compared with optical validation data, and RMSE between 0.2 and 0.7 m between model and field validation data. This allowed for characterizing the distribution and dynamics of 4 marsh wetlands hydroperiod classes, temporary, seasonal, semipermanent, and permanent, and mapping of the sequential vegetation bands that included emergent, obligate wetland, facultative wetland, and upland plant communities. Hydroperiod variation and surface water extent were found to be influenced by short-term rainfall events in both wet and dry years. Seasonal hydroperiods in wetlands were particularly variable if there was a decrease in the temporary or semipermanent hydroperiod classes. In years with extreme rain events, the temporary wetlands especially increased relative to longer lasting wetlands (84% in 2015 with significant rainfall events, compared with 42% otherwise).

KEYWORDS

frequency analysis, hydroperiod, synthetic aperture radar (SAR), time series, vegetation, wetlands

1 | INTRODUCTION

Wetlands are vital for replenishing and storing groundwater, preventing flooding, reducing erosion, filtering and purifying water, and storing substantial amounts of carbon (Kettridge & Waddington, 2013; Turetsky et al., 2011). Prairie potholes are depressions formed after glacial retreat in the last ice age (~12,000 years ago), promoting wetland formation in these depressions (Winter, 1989). They are classified by Stewart and Kantrud (1971) and Cowardin, Carter, Golet, and LaRoe (1979) as marsh wetlands having less than 1-m water depth at peak volume, with vegetation and surface water cover being the indicators of marsh type and permanency. Prairie pothole wetland water levels and extent can fluctuate daily, seasonally, and unpredictably following prolonged periods of rainfall, affecting the ecological characteristics of a wetland controlled by the presence and duration of open water, referred to as the "hydroperiod" (Ewel, 1990; Mitsch & Gosselink, 2007).

As these freshwater resources become increasingly scarce, there is a need for improved wetland monitoring and management through mapping and inventory (Ozesmi & Bauer, 2002). Changes in the water balance are driven by changes in the input (precipitation) and the primary output (actual evapotranspiration), which is driven by air temperatures and other factors (Milly & Dunne, 2011, 2016). There are trends in net radiation (Wild, 2009), vapour pressure (Willett, Jones, Gillett, & Thorne, 2008), and wind speed (McVicar et al., 2012) that also influence water balance. Furthermore, warmer temperatures and reduced precipitation trends are causing drying of wetland surface and groundwater, resulting in changes to hydrology and vegetation (Klein, Berg, & Dial, 2005; Riordan, Verbyla, & McGuire, 2006; Roulet, 2000). Although policy makers have sufficient scientific information to understand the need to take steps toward conservation, the global extent and spatial scale of wetlands are immense. Traditional mapping methods require significant amounts of in situ data collection, which can be logistically challenging and costly and may omit or underestimate the extents of many smaller seasonal or annual wetlands (Frey & Smith, 2007; Halsey et al., 2004). Therefore, governing entities increasingly rely on developing remote sensing techniques to quantify wetland changes for water monitoring and management, where changes can be tied to ecosystem function using in situ validation methods.

1.1 | Remote sensing for water mask generation

Remote sensing application domains use spatial and temporal data covering large areas that are not geographically limited by in situ access and include flood extent delineation, habitat mapping, and wetland assessments that have been found to greatly enhance water resources monitoring, ecological studies, and infrastructure management (Brisco et al., 2017; Irwin, Beaulne, Braun, & Fotopoulos, 2017; Ozesmi & Bauer, 2002).

Synthetic aperture radar (SAR) backscatter signals have been commonly used for surface water extraction (Brisco, 2015; Schlaffer, Chini, Dettmering, & Wagner, 2016; White, Brisco, Pregitzer, Tedford, & Boychuck, 2014), having two distinct benefits for earth observation applications: (a) Radar systems can collect any time of day or night and under poor weather or atmospheric conditions, and (b) backscatter (radar reflections) provide different information to optical sensors. High spatial resolution (1–5 m) modes from RADARSAT-2 have been used to monitor small wetlands and enhance discrimination between land and water allowing for better characterization and classification of wetlands (Brisco, 2015; Schmitt, Liechtle, & Roth, 2012; White et al., 2014). Open water areas have a high dielectric constant and act as a specular reflector under calm conditions causing very little backscatter to the sensor; therefore, water appears dark (Di Baldassarre, Shucmann, Brandimarte, & Bates, 2011). Based on this, several water boundary extraction algorithms have been developed using pixel, object based, or threshold classification approaches (Bolanos, Stiff, Brisco, & Pietroniro, 2016; Brisco, 2015; Martinis, Kuenzer, Wendleder, & Dech, 2015).

1.2 | Wetland classification system

While the combination of several wetland classification systems (regionally variable) enhances and clarifies wetland classification, Stewart and Kantrud (1971) and Cowardin et al. (1979) are foundational documents used for most marsh wetland assessments in the PPR of North America (USA and Canada). Marshes are divided into five different types based on open water and vegetation zones (Figure 1). Each of these zones is subject to variable water levels and vegetation succession depending on snowpack melt and rainfall. Class I is highly variable, generally not displaying surface water, and has little associated ecological or monetary value compared with the other classes (II to V; Alberta Environment and Sustainable Resource

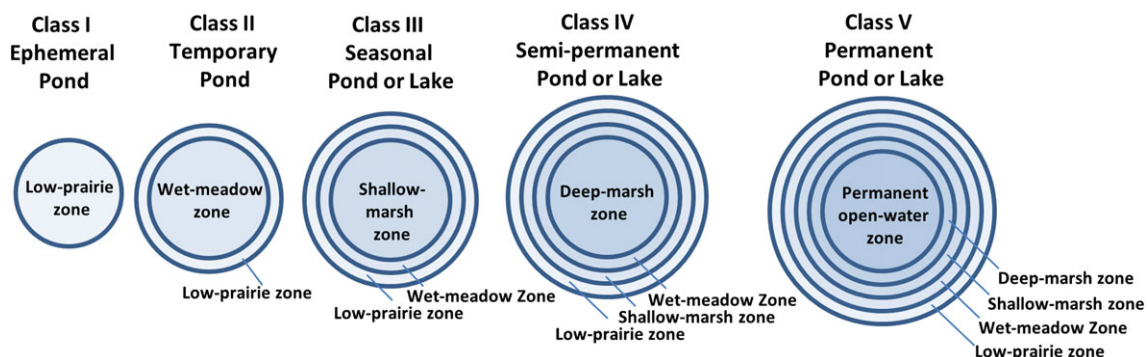


FIGURE 1 Marsh wetland classifications based on water permanence and spatial relation of associated wetland riparian zones. Adapted from Stewart and Kantrud (1971)

Development (ESRD, 2015); therefore, it is excluded from the study. Hydroperiod of the four marsh wetland types (Table 1) is indicative of how permanent the wetland is both seasonally and annually (Ameli & Creed, 2017; Kantrud, Millar, & Van Der Valk, 1989; Stewart & Kantrud, 1971). Semipermanent and permanent wetland types have been merged into one class because of the limited 3-year data series (certainty of permanent [V] wetlands requires a longer time frame).

1.3 | Objective

This study examines how high-resolution, C-HH (horizontal transmit and return to sensor) SAR data can be utilized to classify dynamic marsh and shallow-open water wetlands by associating surface water extent and permanence. Objectives of the study were to (a) present and evaluate an effective approach to derive water masks from SAR imagery and compare them to water masks derived from temporally similar optical imagery and (b) classify open water wetland hydroperiod and permanence using frequency analysis over a 3-year time period.

2 | MATERIALS AND METHODS

2.1 | Study area

The Shepard Slough study site is located along the western boundary of the PPR (Figure 2) in a 278-km² polygon east of the City of Calgary,

Alberta, Canada (Figure 2b). Shepard Slough is characterized as an urban fringe, suburban, agri-human, and agricultural, modified prairie pothole environment in the grassland natural region, with gently rolling plains dominated by moderately calcareous glacial tills at an average elevation of 1,030 m (Natural Regions Committee, 2006).

Four wetland study sites are examined, identified by defining landscape features or proximity to existing wetland monitoring infrastructure: “West Chestermere” (Figure 2c) and “Pumpjack” (Figure 2d) are individual wetlands in agricultural fields in well-defined depressions (determined from a Lidar DEM). “Algae” (Figure 2e) and “Pothole” (Figure 2f) are larger spatial scale areas containing many individual hydrologically variable wetland components in dynamic prairie pothole landscapes. These latter two wetland areas are more disconnected from surface hydrological inflows due to upstream flow diversions. The differences in hydrological drainage characteristics and spatial coverage between the wetland focus areas were chosen to evaluate the utility and effectiveness of the presented hydroperiod analysis over a range of scales and wetland types.

2.2 | Synthetic aperture radar

RADARSAT-2 SAR data were collected at each repeat cycle (24 days) in 2013 to 2015 during the ice-off season. Eighteen (six each year, [Table 2]) Ultra-Fine (U77) single look complex 20 × 20 km swath

TABLE 1 Marsh hydroperiod and defining vegetation zone based on the Stewart and Kantrud (S&K) (1971) wetland classification system

Wetland type (S&K)	Hydroperiod	Vegetation zone
Temporary (II)	Surface water present for short time after snowmelt or heavy rainfall.	Wet meadow
Seasonal (III)	Surface water present throughout growing season, dry by end of summer.	Shallow wetland
Semipermanent (IV)	Surface water is present for most or all the year, except in drought conditions.	Deep wetland
Permanent (V)	Surface water present throughout year.	Open water

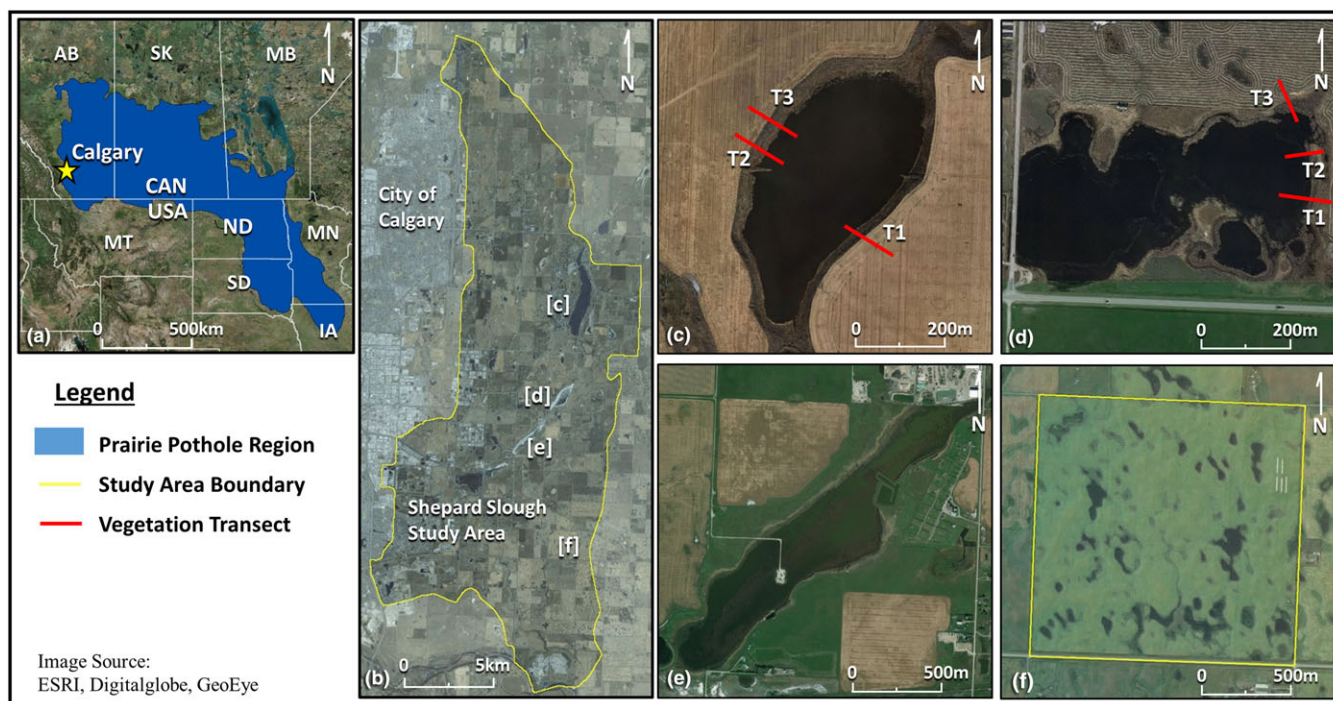


FIGURE 2 (a) PPR in Canada and USA; (b) Shepard Slough case study area ~10 × 30 km adjacent to Calgary, Alberta; (c) West Chestermere; (d) Pumpjack; (e) Algae; and (f) Pothole. Vegetation transects surveyed in 2015 are shown as red in (c) and (d)

images in ascending orbit, approximately equally spaced through the vegetation growth season from April through August/September, are used to derive surface water masks, with a nominal resolution of 2.8×2.8 m (Macdonald and Dettwiler and Associates Ltd, 2016). Although the nominal resolution of the U77 mode SAR is 2.8×2.8 m, the SAR dataset was resampled to 5×5 m to match the optical datasets spatial resolution (5×5 m) for validation purposes. The SAR image from June 2015 had significant quality issues. Therefore, to maintain consistent sample size ($n = 6$) for each year, an acquisition from June 7, 2016, was substituted based on similar environmental conditions (0 mm precipitation, Figure 6).

2.3 | Optical

RapidEye (Planet Labs) optical image data from May 8, 2014, and Satellite Pour l'Observation de la Terre (SPOT) (*Centre national d'études spatiales*) from July 15, 2015, and September 20, 2015, sampled at 5×5 m resolution were acquired on near-coincident or coincident days as some of the SAR data for validation purposes. All images were atmospherically corrected. Surface water in all optical images was classified using K-means unsupervised classification (Burrough, Gaans, & MacMillan, 2000; Burrough, Wilson, & van Gaans, 2001; Lane et al., 2014).

2.4 | Lidar

Airborne Lidar data were collected by Airborne Imaging (Calgary, Canada) in 2008 over the Shepard Slough area. Processing of a bare earth $1 \text{ m} \times 1 \text{ m}$ digital elevation model (DEM) was conducted following the methods of Hopkinson et al. (2005). The Lidar DEM was used for orthorectification of the SAR and optical data and provided topographic validation for water surfaces within wetland basins while illustrating the surface hydrologic flow pathways for the study area.

2.5 | Ground validation

Wetlands were chosen for the study from preexisting GoA stilling wells and a series of optical images based on apparent riparian disturbance (Figures 2c–f). Of the four chosen study locations, two were visited in the last week of July 2015 to determine surface water extent and riparian habitat boundaries using a Global Navigation Satellite System (Topcon HiPer SR (Livermore, CA, USA)) to centimetre accuracy. Positions were differentially corrected to a static base station using precise point positioning. Cross-sectional transects

TABLE 2 Ultra-Fine (U77) synthetic aperture radar acquisition dates at Shepard Slough for 2013 to 2015 (2016)

2013	2014	2015
April 19	April 14	April 9
May 13	May 8	May 3
June 6	June 1	June 7 (2016)
June 30	June 25	—
July 24	July 19	July 14
August 17	August 12	August 31
—	—	September 24

were established extending perpendicularly away from the shorelines and upwards from the wetlands to reflect vegetation zones and changes in vegetation community composition. For each vegetation band, the predominant plant species were identified, with abundance ranking by estimated foliar cover. Common names, taxonomic treatment, and life history characteristics are in accordance with USDA-Plants (United States Department of Agriculture, Natural Resources Conservation Service; <https://plants.usda.gov/java/>), with some wetland characteristics for a few species from Washington State Department of Transportation lists (wsdot.wa.gov).

2.6 | Surface water extraction

A surface water threshold intensity/decibel (dB) extraction method developed by White et al. (2014) was updated with current filter and dB modules to extract surface water. Figure 3 presents a flow diagram of the image processing, surface water extraction, and frequency analysis workflow. Images are calibrated to sigma naught (σ), converted from linear to decibel, then filtered to reduce the amount of speckle before applying a threshold value to the image, maintaining spatial resolution and edges (Schmitt & Brisco, 2013; White et al., 2014). The FGAMMA (gamma) adaptive filter is used to preserve edges to maintain water extent (Toutin, 2011; Zhang et al., 2012). The FAV (averaging mean filter) filter is used to reduce speckle and noise, and the FMO filter is used to further reduce noise and has been found to help with the orthorectification (White, Brisco, Daboor, Schmitt, & Pratt, 2015). FGAMMA and FAV filters are applied independently in parallel, to avoid the possibility of compounded loss of water edge detail, then combined later in the routine (White et al., 2014).

Extraction of the threshold decibel (dB) ranges that represent surface water was sampled over a consistent area polygon (70 ha in area [28,000 pixels]) at Chestermere Lake, which is a controlled reservoir. The threshold (dB) sampling routine (95th percentile) is presented as a manual process in this study, and the values are scene specific due to weather effects on the backscattering but can be automated based on training data or other surface water inventories (Peiman, Husam, Brisco, & Hopkinson, 2016). Pixels not selected as surface water after the FAV filter and not in FGAMMA are then not included as open water to again preserve edges (White et al., 2014). Orthorectification to the 2008 Lidar DEM was performed in using rational function and metadata ground control points.

2.7 | Hydroperiod Analysis

A measure of water permanence and hydroperiod throughout the growing season is performed using an “equals frequency” routine on the six-binary surface water raster images for each year (Figure 4a), calculating the number of times a pixel is identified as water in the same geographic location (Figure 4b). Reference rasters contain a numerical pixel value that corresponds to the water pixel values in the input rasters. Input rasters are binary and contain only “0” (*land*) and “1” (*water*) values (Figure 4b). Reference rasters were created by mosaicing all input water mask rasters into a new mask with only “1” (*water*) values of the maximum extent of all input water mask rasters. All water masks were clipped to the reference raster to

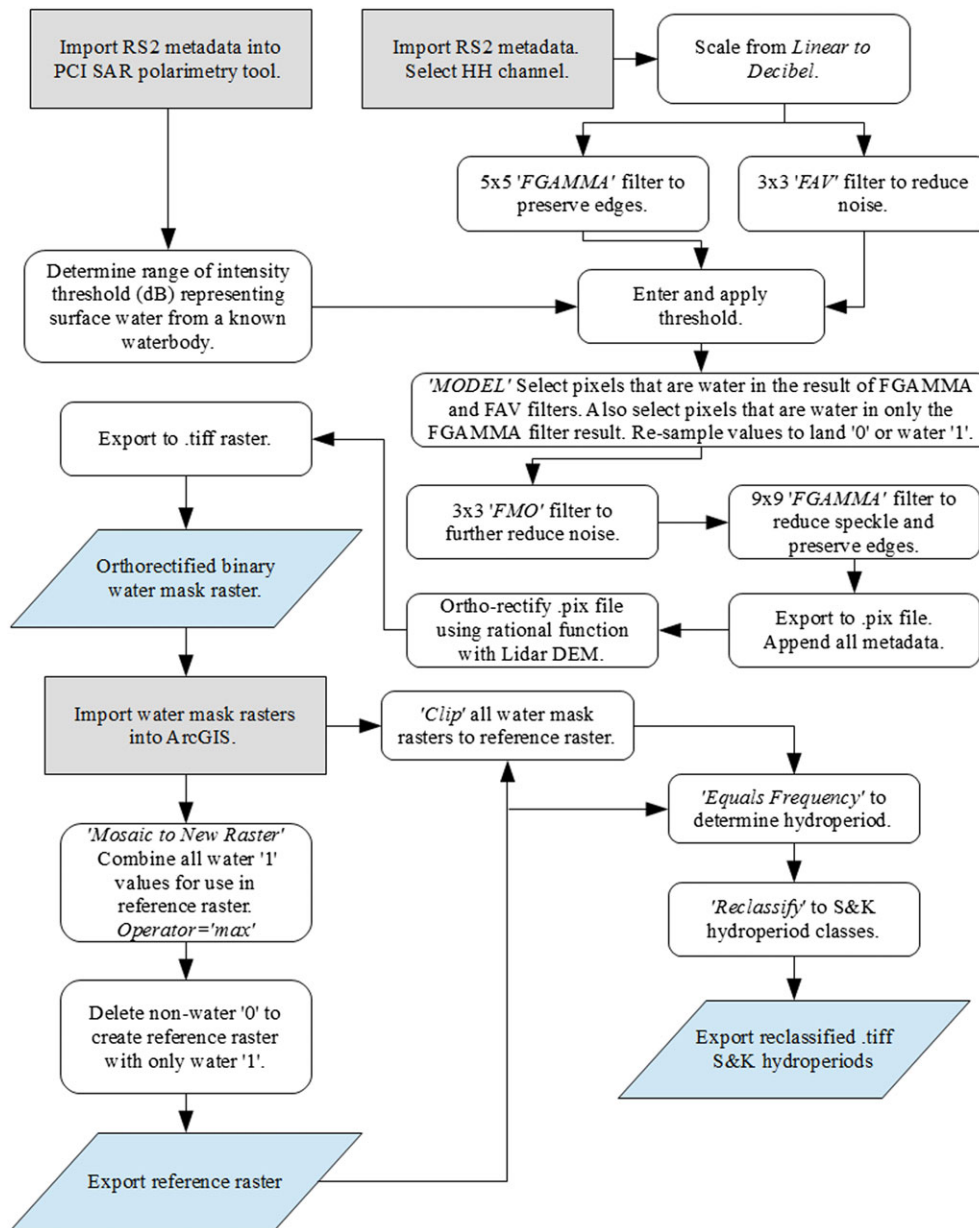


FIGURE 3 Flow diagram of intensity (dB) threshold routine to create binary water masks and hydroperiod classification. Grey rectangles indicate inputs, white icons are intermediate processes, and blue parallelograms represent final outputs. Software functions are italicized. DEM = digital elevation model; SAR = synthetic aperture radar

avoid commission of land before executing the equals frequency routine.

The output pixel frequency corresponds to the number of months ($n = 6$) used in each year (Figure 4c) then reclassified from frequency values (1 to 6) to hydroperiod (Figure 4d), where 1–2 months represents “temporary” (S&K Class II), 3–4 months is “seasonal” (S&K Class III), and 5–6 months is “semipermanent/permanent” (S&K Classes IV and V), based upon Stewart and Kantrud (1971) and Cowardin et al. (1979; Table 1). Wetlands that exist year round were not differentiated from semipermanent in this study because SAR cannot directly detect water under winter snow and ice conditions, and thus, the certainty of a permanent (class V) wetland is uncertain. Consequently, class V (permanent water bodies) constitute a subset of class IV wetlands in this study.

3 | RESULTS

3.1 | SAR binary water mask extraction

Results indicate that the intensity thresholding technique developed by White et al. (2014) is effective for extracting surface water of large and small wetlands in a dynamic prairie pothole marsh environment (Figure 5). The average upper dB threshold limit was found to be -14 dB, and the lower limit -31 dB, with dB ranges varying with weather and ground conditions (Table 3 and Figure 6). May 13, 2013, and August 31, 2015, outputs were found to be of poor quality for surface water extraction due to high backscatter from waves associated with high winds (gusts up to 67 and 57 kph, respectively, Table 3), resulting in similar dB ranges in water bodies as surrounding

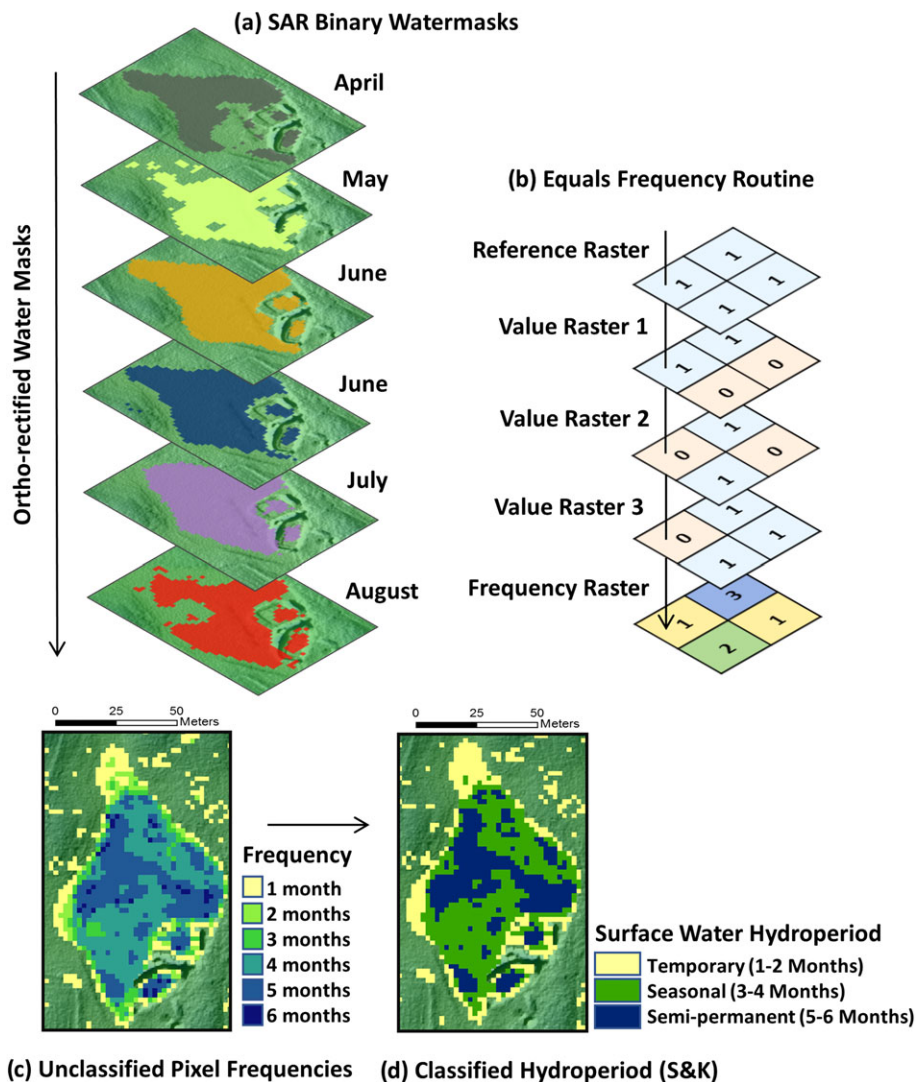


FIGURE 4 Visual flow diagrams of (a) binary water mask stacking; (b) equals frequency routine; (c) unclassified pixel frequency output; and (d) hydroperiod classification. Binary water masks and hydroperiod rasters overlay a lidar digital elevation model for visualization purposes. SAR = synthetic aperture radar

areas of known land. Notable change in surface water extent of larger wetland areas is seen in these images, compared with smaller wetlands.

3.2 | SAR and optical validation

Ten optical mask classifications of RapidEye and SPOT images were tested for classification accuracy based on training areas, with overall optical classification accuracies ranging from 87% to 95%, and Kappa values ranging 0.72 to 0.87. SAR and optical water masks were compared using two sets of near-coincident acquisitions (within 4 days) and one set of temporally coincident (May 8, 2014; Figure 7), presenting positive correlations of 76.6% to 92.1% (Table 4).

3.3 | Field validation

Pumpjack and West Chestermere are wetlands that have minimal agricultural disturbance from activities such as tilling, allowing for riparian vegetation growth, validated from riparian vegetation

composition and abundance during field data collection (Figure 8b; Tables 5 and 6). The RMSE of the riparian transects and water extent observed in field validation data and optical data were between 0.2 and 0.7 m, less than 10% error between field and model, or approximately 0.5 m.

A mixture of native species and extensive occurrence of introduced plants was observed at all sites, generally associated with the prairie agricultural regions, with some weedy and invasive species (Table 6). Indicator plant species include duckweed, cattail, sedges, managragass, and reed canary grass, which characterize inundation patterns and summer positions above the groundwater table, vegetation zones, and hydroperiod. Based on the vegetation species composition and zones observed at both wetlands, the habitat zones are classified as follows: H5, aquatic open water; H4, deep marsh zone; H3, shallow marsh zone emergent plants and obligate wetland species; H2, wet meadow zone with facultative wetland species; and H1, low prairie zone with facultative upland plants. These habitat zones correspond to those found in a Classes IV or V marsh wetland described by Stewart and Kantrud (1971; Figure 1). Five indicator ratings based on

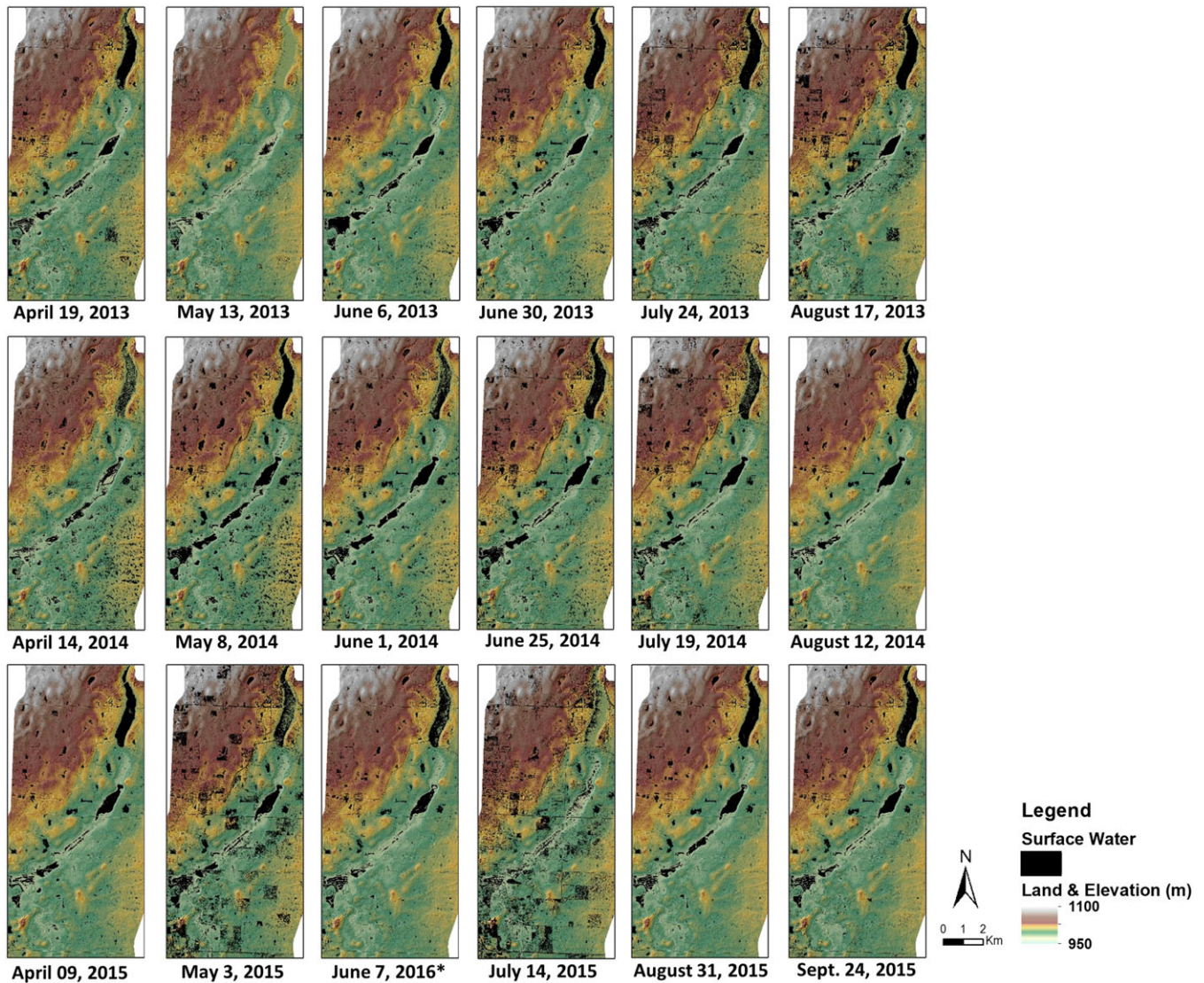


FIGURE 5 Synthetic aperture radar derived surface water masks using the intensity (dB) thresholding approach for 2013 (top row), 2014 (middle), and 2015 (bottom). Images show the dynamic changes of wetland surface water over the growing season at Shepard Slough. Note that quality issues with May 13, 2013; August 31, 2015; and that June 7, 2016 are substituted for June 2015

Lichvar, Melvin, Butterwick, and Kirchner (2012) designate the preference of a plant species' occurrence in a wetland environment, ranging from "obligate wetland," being the highest preference for wetland environments, to "obligate upland," being the lowest preference in wetlands (Table 7). The entire range of indicator species is represented in the vegetation zones observed at Pumpjack and West Chestermere (Tables 5 and 6).

Some apparent unique vegetation banding was observed (duckweed communities at Pumpjack, transect two), but overlap of species was observed across the sequential vegetation zones at each wetland (foxtail barley and smooth brome). Reasonable consistency for multiple transects within sites was observed, with some consistency of indicator species across the two wetland sites (mannagrass and sedges).

3.4 | Wetland hydroperiod frequency analysis

Wetland hydroperiod classification results and associated area of each hydroperiod class in hectares are detailed for each year

(2013–2015) at the four study sites, presented in Figure 9. SAR acquisition date, daily precipitation, and temperature information from the Calgary International Airport weather station, the closest weather station to the study area, are detailed in (Figure 6). Precipitation over the study period (April–September) for each year is as follows: 2013 = 384 mm, 2014 = 289 mm, and 2015 = 310 mm (118 mm in late August), compared with an average of 346 mm over the same months from 2007 to 2016. Notable rainfall events are seen in May and June of 2013, as well as August and September of 2015. For both well-defined basin wetlands (Pumpjack and West Chestermere), less open water is observed in 2013, which was the year with the most precipitation (West Chestermere has 11.5 ha in 2013, compared with 13.9 ha in 2014, and 14.7 ha in 2015; Pumpjack has 16.3 ha in 2013, 20.0 ha in 2014, and 17.8 ha in 2015), whereas pothole area wetlands (Algae and Pothole), somewhat counterintuitively, do not follow the same trend, potentially due to differences in riparian vegetation growth, and wetland shape and size (Figure 9), or perhaps is a constraint of the Radarsat-2 24-day repeat imaging interval.

TABLE 3 Confusion matrix of near-coincident SAR and optical (RapidEye and SPOT) data from 2014 and 2015

Acquisition date (yyyy-mm-dd)	Upper limit (dB)	Lower limit (dB)	dB range percentage (%) of pixels used from sample area	Wind/gust speed (km/hr)	Daily precipitation (mm)
2013-04-19	-16	-30	89	21/no data	1-cm snow
2013-05-13	-18	-32	89	28/67	Trace rain
2013-06-06	-17	-30	90	23/43	Trace rain
2013-06-30	-15	-28	85	15/35	0
2013-07-24	-13	-30	85	14/31	0.8
2013-08-17	-18	-32	90	14/50	0.6
2014-04-14	-9	-25	89	20/37	0
2014-05-08	-15	-30	85	34/44	0
2014-06-01	-8	-28	94	13/46	5.4
2014-06-25	-14	-30	86	14/57	2.1
2014-07-19	-15	-32	90	17/31	No data
2014-08-12	-14	-32	90	27/48	0
2015-04-09	-15	-33	85	13/31	0
2015-05-03	-15	-32	92	5/35	Trace rain
2016-06-07	-15	-30	88	34/44	0
2015-07-14	-8	-31	90	19/52	0.4
2015-08-31	-10	-30	88	12/57	0
2015-09-24	-17	-33	88	16/35	0
Average	-14	-31	89	19/44	—

Note. Results do not represent absolute accuracies, as optical water masks contain some uncertainty, and the two weaker comparison results represent acquisitions from different days.

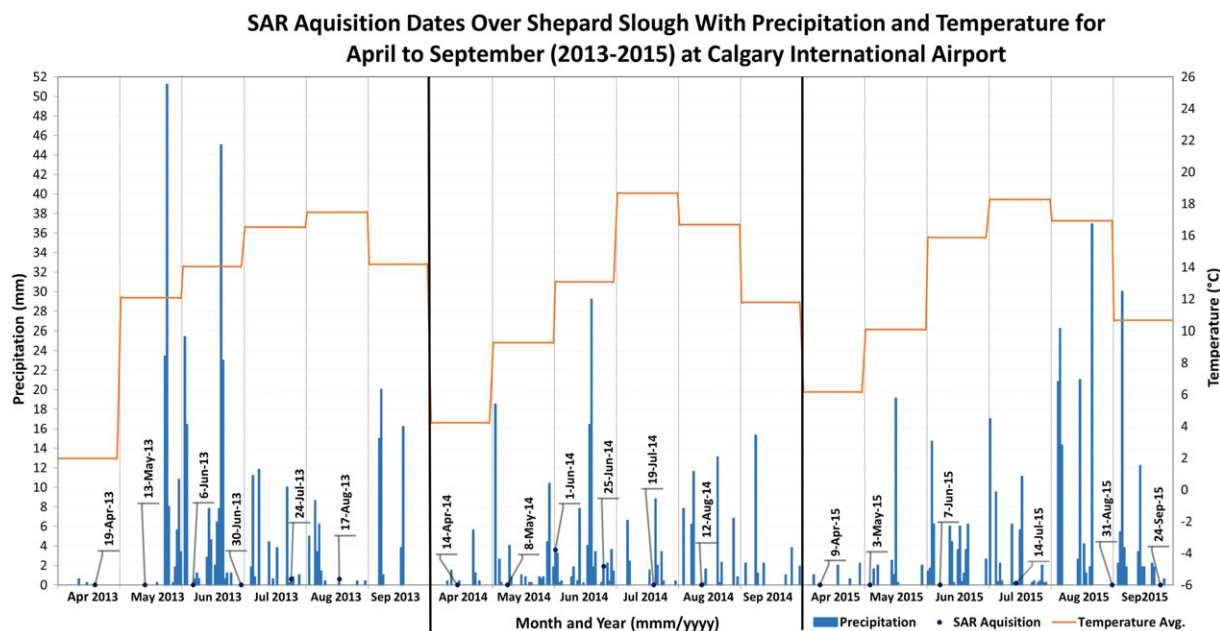


FIGURE 6 Meteorological data with monthly average temperature and daily precipitation for Shepard Slough recorded at the Calgary International Airport. Note that total precipitation for June 7, 2016, was the same as June 7, 2015, at 0 mm. SAR = synthetic aperture radar

Seasonal hydroperiod class fluctuations are identified in hydroperiod histograms detailing hydroperiod classes by year (Figure 10). The seasonal hydroperiod is found to be more variable than temporary and semipermanent in both “Algae” and “Pothole,” whereas the semipermanent/permanent hydroperiod is most variable in the defined basin wetlands of Pumpjack and West Chestermere. This indicates isolated

pothole wetland hydroperiods are more spatially variable than deeper wetlands in defined basins with surface hydrological connectivity or downstream flow obstruction.

West Chestermere similarly to Pumpjack is contained in a well-defined moderate-sized catch basin and has similar hydroperiod patterns. One difference is the spike in seasonal hydroperiod in 2013,

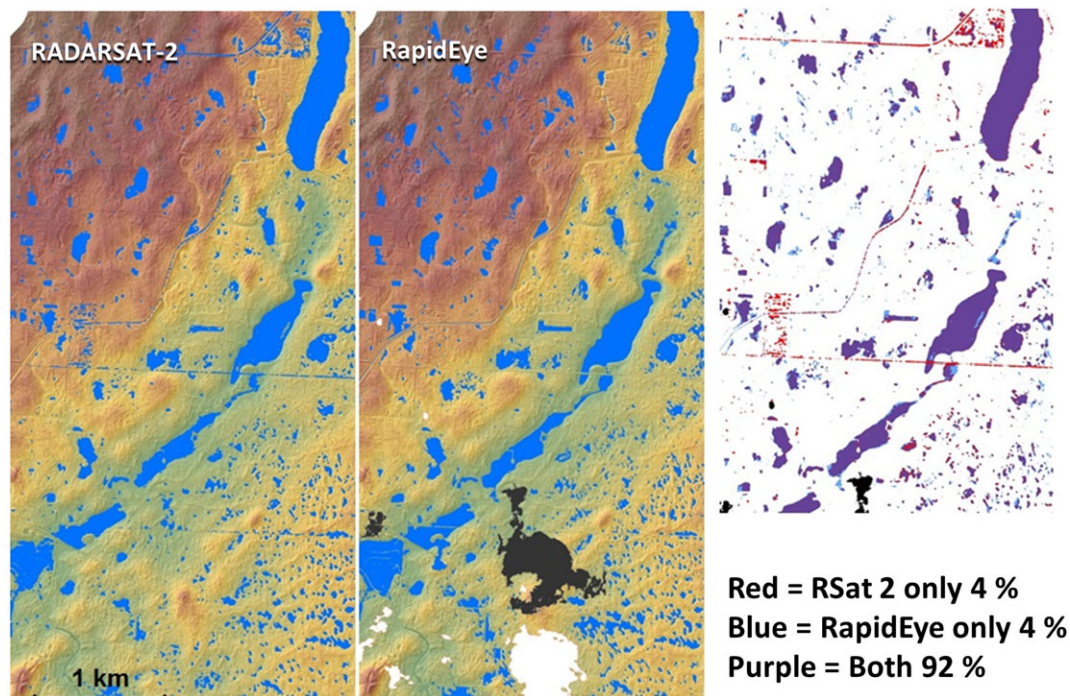


FIGURE 7 Comparison of binary water masks for temporally coincident SAR (left) and RapidEye (middle) on May 8, 2014. Cloud (white) and shadow (black) are shown in the RapidEye image. Correlation (right) shows areas of agreement in purple, SAR only as red, and RapidEye only as blue. SAR = synthetic aperture radar

TABLE 4 SAR acquisition dates and surface water intensity decibel (dB) ranges, with associated pixel contributions

SAR date	Optical date	True positive	False positive	Misclassification rate	Overall (%)
2014/05/08	2014/05/08	92.1	0.5	0.3	95.2
2015/07/15	2015/07/14	76.5	1.2	4.7	88.7
2015/09/24	2015/09/20	84.8	2.9	1.4	96.1

Note. Wind (km/hr) and daily precipitation (mm) information from the Calgary, Alberta International Airport is also provided. SAR = synthetic aperture radar.

resulting in more seasonal than semipermanent hydroperiod at over 5 ha, compared with 2–3 ha observed in 2014 and 2015. Higher variation from the mean is seen in the semipermanent class at Pumpjack and west Chestermere. Lower variation from the mean is seen in the seasonal class at Algae and Pothole (Figure 9). Hydroperiod fluctuations occur frequently and have inconsistent duration in “Algae” and “Pothole” study areas where rain events (Figure 6) contribute disproportionate temporary hydroperiod (Figure 10), even in a drought year (2015) where many temporary hydroperiod pixels are found in areas along roadways (ditches) and shallow depressions on the landscape (Figure 9). This variability in per-pixel hydroperiod class is moderated in Pumpjack and West Chestermere, presumably because of increased surrounding hydrological connectivity (West Chestermere) or diminished opportunity for surface drainage (Pumpjack).

4 | DISCUSSION

4.1 | Riparian vegetation and hydroperiod variation

Wetlands with predominantly semipermanent hydroperiods may contain fewer riparian vegetation species because of more consistent surface water extents (Figure 10). This is mostly reflected in deep

wetland, and aquatic habitat zones because of reduced variation from the semipermanent hydroperiod (Table 5). Semipermanent or permanent marsh wetlands surrounded by temporary hydroperiods may promote greater ecological diversity, described in Stewart and Kantrud (1971). Consistently similar ratios between the three hydroperiod classes each year and presence of each hydroperiod observed at Pumpjack indicate low class variability and stable conditions across the 3 years studied (temporary, 3 to 4 ha; seasonal, 3 to 4.5 ha; semipermanent, 10 to 13 ha). The most noticeable difference in surface water extent is seen in the northeast corner of “Pumpjack” (Figure 9), which is dominated by common cattail (*Typha latifolia*). In images from 2013 and 2014, this band of cattail is easily identifiable, appearing as elevated topography (1–2 m height) adjacent to the surface water. In 2015, however, this area is inundated by temporary surface water. This inundation would reduce the vigour and density of these cattails, and this emergent plant is subject to seasonal die-off as reported by Brisco et al. (2017) in similar vegetated wetland environments.

Open water can be covered by varying extents of emergent and floating aquatic vegetation during certain growth stages throughout the year (Brisco et al., 2017). Significant rain events on May 23–24, 2013 (74 mm), and June 2–3 in 2013 (42 mm) likely promoted riparian and emergent vegetation growth earlier in the growing

FIGURE 8 Wetland vegetation and water extent field transects collected in July 2015 near-coincident with SAR acquisition over: (a) Pumpjack (Transect 3, Table 5) and (b) West Chestermere (Transect 2, Table 5). Green points indicate field points. RapidEye vegetation zone colours have not been reclassified to represent a particular zone, therefore just indicate where general zones transition along transects. SAR = synthetic aperture radar

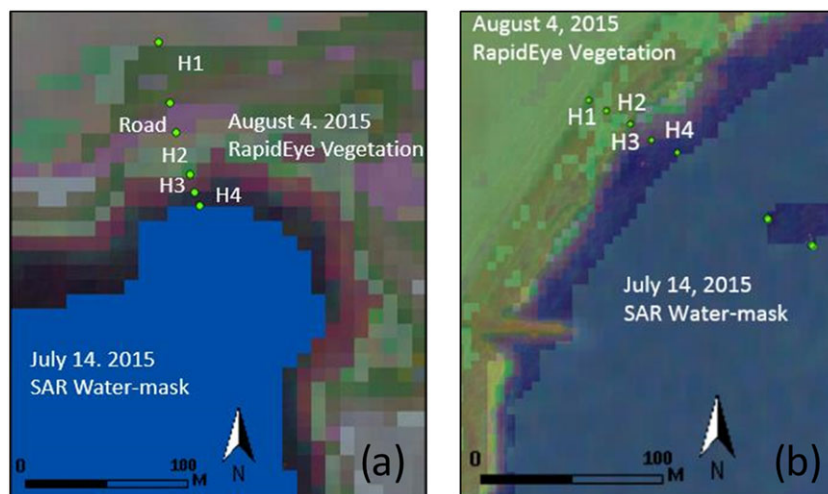


TABLE 5 Riparian vegetation species transects for Pumpjack and West Chestermere

Wetland Transect	Habitat zone	Plants sequenced by decreasing abundance	
Pumpjack			
1	H1	Foxtail, sowthistle, goosefoot, mannagrass, cattail	
	H2	Goosefoot, cattail	
	H3	Cattail, buttercup	
	H4		
2	H1	Foxtail, cattail	
	H2	Foxtail, goosefoot, sloughgrass, cattail, mannagrass	
	H3	Goosefoot, bur-reed, dandelion	
	H4/5	Duckweed	
3	H1	Duckweed	
	H2	Foxtail	
	H3	Foxtail, sloughgrass, sedges	
	H4	Buttercup, goosefoot, cattail, bulrush	
	H4	Lamb's quarter, dandelion, goosefoot, ranunculus	
	West Chestermere		
	1	1	Brome, rush, dandelion, sowthistle
		2	Sedges, foxtail, quackgrass, rush
3		Mannagrass, foxtail	
4		Foxtail, goosefoot, manna grass	
2	1	Brome, reed, wheatgrass, wildrye	
	2	Foxtail, manna grass, sedges	
	3	Manna grass, spikerush, sedges	
	4	Sedges	
3	1	Brome, reed canary grass, wheatgrass, wildrye	
	2	Foxtail, manna grass, sedges	
	3	Mannagrass, spikerush, sedges	
	4	Sedges	

Note. Refer to Figure 2c,d for transect locations. Transect 3 is seen in Figure 8.

season, resulting in less open water being identified by the threshold routine, which does not recognize flooded vegetation as a clear unobstructed open water surface (Brisco et al., 2017; White et al., 2014). Wetland surface water extent was found to change dynamically, corresponding to rainfall occurring seasonally or annually. This effect is seen in both “Algae” and “Pothole” where an increase in temporary hydroperiod is related to precipitation events in May–June 2013 and August–September 2015. In the year with the closest to “normal” (2014) rainfall magnitude and frequency, a sharp increase

in seasonal hydroperiod of pothole wetlands (algae [2013 = 15 ha, 2014 = 32 ha, and 2015 = 12 ha] and pothole [2013 = 12 ha, 2014 = 18 ha, and 2015 = 2 ha]) is observed, suggesting these wetlands experience an overall increase in water area, but also transition to a seasonal hydroperiod from either temporary or semipermanent in comparatively dry or wet years.

Most notable is the variation from the mean of hydroperiod classes in the “Algae” semipermanent hydroperiod (Figure 11). In the 2013 wet year, there is 33% more semipermanent water compared with the

TABLE 6 Most common plant species around the Pumpjack and West Chestermere wetlands, sequenced by decreasing occurrence across transect habitat zones

Rank occurrence	Common name*	Scientific name	Native/intro.	Growth	Wetland status	Comment
1 (48%)	Foxtail barley	<i>Hordeum jubatum</i> L.	N (hybrid)	Graminoid	Facultative	Generalist – weed hybrid
2 (35%)	Sedges, inc. beaked sedge	<i>Carex</i> sp., including <i>C. rostrata</i> Stokes	N	Graminoid	Obligate wetland	Specialists, hydrophytic
3 (30%)	Mapleleaf goosefoot	<i>Chenopodium simplex</i> (Torr.)R	N	Forb	Upland	Disturbance promoted
4 (30%)	American mannagrass	<i>Glyceria grandis</i> S. Watson	N	Graminoid	Obligate wetland	Short/tall to 1.5 m
5 (26%)	Broadleaf cattail	<i>Typha latifolia</i> L.	N	Forb	Obligate wetland	Often emergent
6 (17%)	Tall buttercup	<i>Ranunculus acris</i> L.	I	Forb	Facultative wetland	Prolific weed
7 (13%)	Common dandelion	<i>Taraxacum officinale</i> F.H. Wigg.	I	Forb	Facultative upland	Widespread weed
8 (13)	Smooth brome	<i>Bromus inermis</i> . Leyss	I	Graminoid	Obligate upland	Weedy or invasive
9 (9%)	Common sowthistle	<i>Sonchus oleraceus</i> L.	I	Forb	Facultative upland	Noxious weed in Alberta
10 (9%)	Reed canary grass	<i>Phalaris arundinacea</i>	N (hybrid)	Graminoid	Facultative wetland	Concern for riparian zone
11 (9%)	Sloughgrass	<i>Beckmannia syzigachne</i> Stued.	N	Graminoid	Obligate wetland	Specialists, hydrophytic
12 (9%)	Western wheatgrass	<i>Agropyron smithii</i> (Rydb.)	N	Graminoid	Facultative upland	Upland regions
13 (9%)	Canada wildrye gras	<i>Elymus</i> sp.	N/I	Graminoid	Facultative upland	Upland regions
14 (9%)	Wire rush	<i>Juncus arcticus</i> Willd.	N	Graminoid	Facultative wetland	specialists, hydrophytic
15 (9%)	Common duckweed	<i>Lemna minor</i> L.	N	Forb/herb	Obligate wetland	Hydrophytic
16 (4%)	Bur-reed	<i>Sparganium</i> L.	N	Forb/herd	Obligate wetland	Often emergent
17 (4%)	Bulrush	<i>Schoenoplectus tabernaemontani</i> (Gmel.)	N	Graminoid	Obligate wetland	Often emergent
18 (4%)	Lamb's quarter	<i>Chenopodium album</i> L.	I	Forb	Facultative	Disturbance promoted
19 (4%)	Quackgrass	<i>Elymus repens</i> (L.) G.	I	Graminoid	Facultative	Weedy or invasive
20 (4%)	Common spikerush	<i>Eleocharis palustris</i> (L) R&S	N	Graminoid	Obligate	Seasonally flooded areas

TABLE 7 Wetland indicator statuses used to designate plant species preference for occurrence in wetland or upland (Lichvar et al., 2012)

Indicator Species	Comment
Obligate wetland	Always occur in wetlands
Facultative wetland	Usually occur in wetlands, but may occur in non-wetlands
Facultative	Occur in wetlands and non-wetlands
Facultative upland	Usually occur in non-wetlands, but may occur in wetland
Obligate upland	Almost never occur in wetlands

3-year mean, whereas in the dry 2015 year, there is 34% less semipermanent water compared with the mean. In 2014, there is only a 0.5% change from the mean over the 3-year study period, suggesting an increase or decrease in overall precipitation in the early growing season (April–June) with inversely related effects on the semipermanent hydroperiod when comparing each year. This trend comparison has potential to be a more widely applicable tool for monitoring that moves away from detailed measurements of local regions and time periods, into a more general measure of variation that provides an index of wetland ecosystem state and function.

4.2 | Data limitations, uncertainties, and future directions

The major limitation of the study relates to temporal image frequency. Because prairie wetlands are hydrologically dynamic (Figures 10 and 11) and heavily influenced by precipitation events (Figure 6), there is a need for increased temporal resolution to better represent short-

term variations in hydroperiod. SAR beam modes other than ultra-fine (U77) such as standard quad (SQ1) could be used to increase the frequency of data collection to enhance the temporal resolution, but each mode has different incidence angles and orbits when collecting data. This results in different backscattering and decibel values between modes due to unique look angles that increases uncertainty of surface water extents. HH polarization of quad or dual polarization data could also be used to extract surface water or emergent vegetation with a trade-off for spatial resolution. Because this study focused on high-resolution monitoring of surface water extents on a per pixel basis, the uncertainties associated with using multiple modes to increase the temporal resolution was considered too great. The C-Band RADARSAT Constellation Mission (RCM) planned for launch in 2018 will offer advanced capabilities for monitoring surface water with high spatial resolution modes (1–3 m), providing enhanced monitoring of smaller wetlands (Canadian Space Agency, 2016). The revisit time of RCM is 4 days (compared with 24 days for RADARSAT-2), allowing for more frequent monitoring and over larger

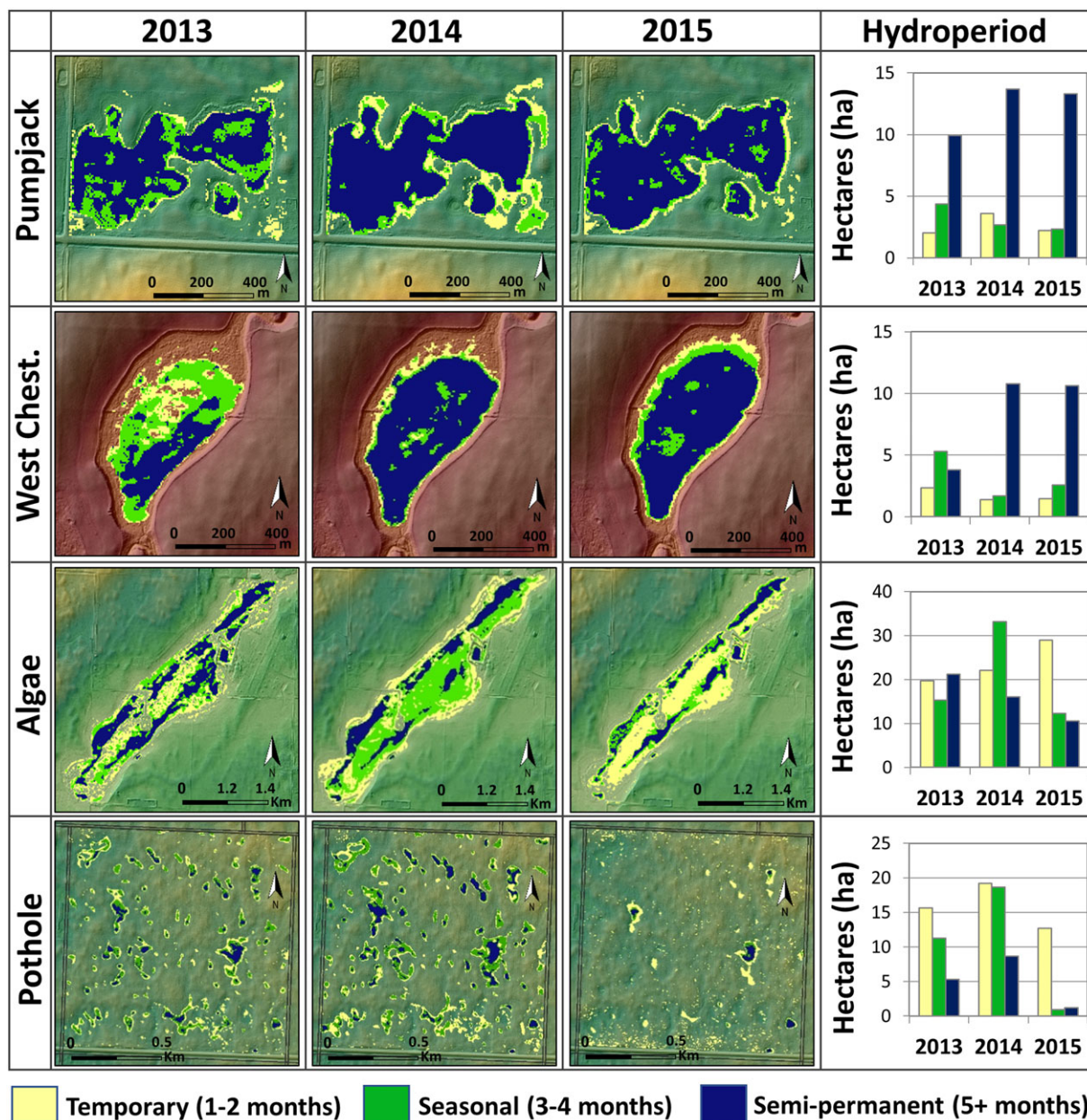


FIGURE 9 Hydroperiod results for Pumpjack, West Chestermere, Algae, and Pothole study areas with associated area in hectares of each hydroperiod. Hydroperiods are shown as yellow for temporary (1–2 months), green for seasonal (3–4 months), and blue for semipermanent/permanent (5–6 months). A lidar digital elevation model is used as the background to illustrate surrounding terrain

areas. Increased temporal resolution has several implications for wetland hydroperiod classification: (a) precipitation events and subsequent local surface water changes will be better represented; (b) weekly hydroperiod comparisons can be made instead of monthly; and (c) increased acquisition frequency will make it easier to find coincident date optical data for comparative validation and data product improvement. This is important for understanding water resources and hydrological variations, especially in ungauged basins.

When a SAR image is acquired in conditions with little wind or surface water roughness, HH has been shown to be the best suited to mapping surface water (White et al., 2014). Although the majority of HH polarization images were found to be of adequate quality for the analysis (Table 3 and Figure 5), some of the images did show significant surface roughness from wind and were therefore unusable for surface water extraction. Although dual polarization data (HH, HV)

was not used, or tested in this study, we see the influence of wind effects in some images (May 3, 2013, and October 31, 2015) that could be mitigated using dual polarization data (White et al., 2014) or, instead, texture-based analysis that works well over some rough water environments (Li & Wang, 2017). Although the consistent sample area polygon reduces the amount of error introduced in the thresholding approach through user selection, uncertainty can still be introduced to the routine when choosing the threshold range from the output dB histogram.

4.3 | Implications of wetland hydroperiod time series

The SAR-derived binary water mask hydroperiod classification described in this study differs from other classification routines, as it combines a series of images into a dynamic surface water hydroperiod

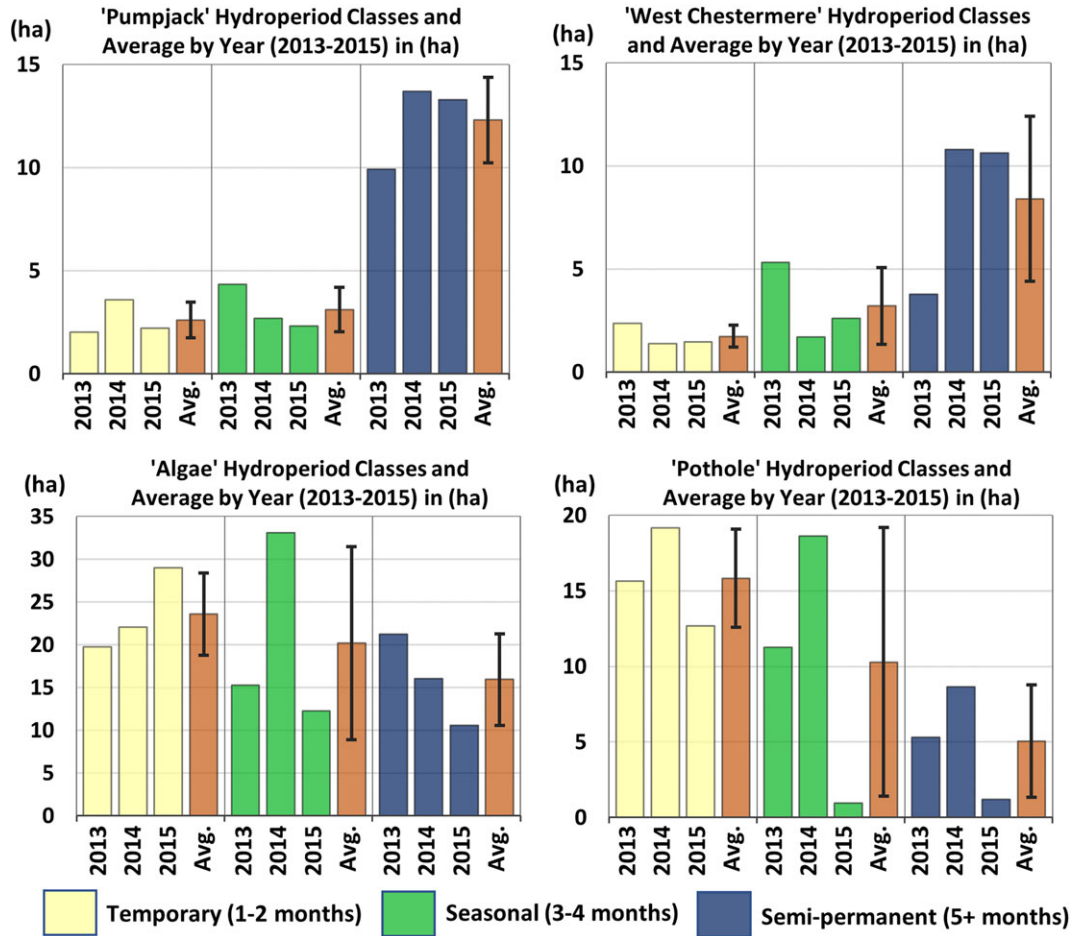


FIGURE 10 Hydroperiod classes grouped by year for each study wetland, showing average and variation of hydroperiod from the mean (orange) for each wetland study site

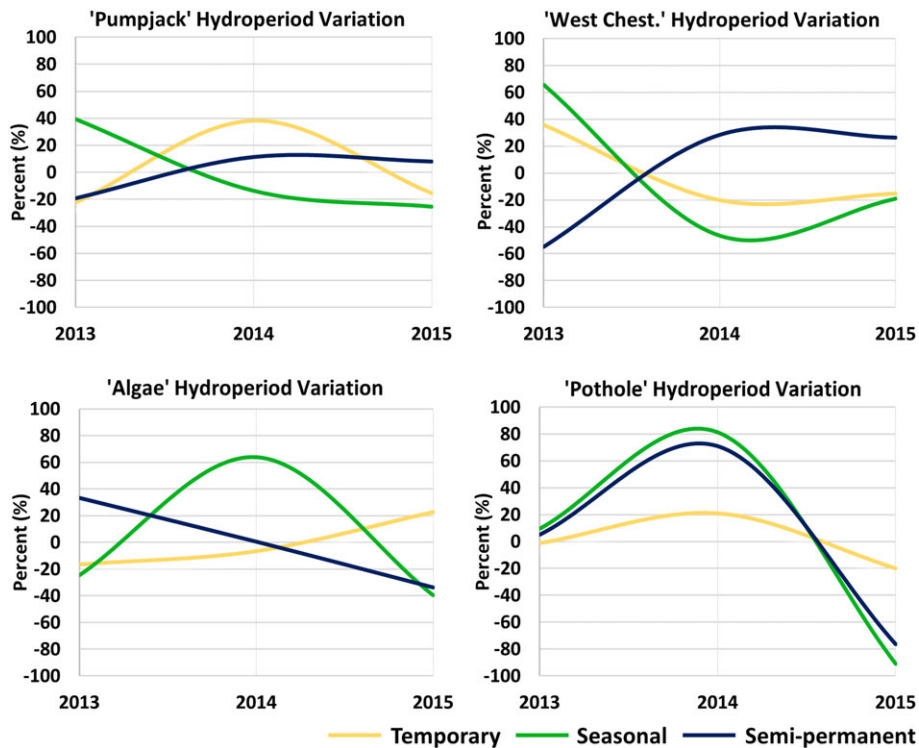


FIGURE 11 Interannual variation (%) of each wetland hydroperiod class from the mean ("0" representing the mean) of each hydroperiod class for each wetland study area from 2013 to 2015

product over the growing season of wetlands, rather than evaluating hydroperiod based on single snapshots in time. The performance and results of the hydroperiod classification may require further evaluation with the greater temporal resolution attained from RCM, in order to perform more rigorous validation. However, the hydroperiod analysis and methodology presented in this study provides a framework for long-term, high-resolution water resource monitoring describing more than just water extent of wetlands, allowing for enhanced characterization and classification of wetlands in accordance with Alberta's provincial wetland classification criteria. It should be noted that the frequency routine could be carried out on any type of data that can produce binary water mask rasters (i.e., optical, Lidar).

5 | CONCLUSION

This study details a framework for a new time-series classification approach based on hydroperiod and hydro-climatic conditions. The frequency analysis and classification based on Stewart and Kantrud (1971) provide a novel method of classifying dynamic marsh environments using temporal SAR data that can be largely automated. Results suggest water mask frequency analysis can be used to determine hydroperiod and permanency of wetlands in the PPR and can potentially be adapted to other environments.

Hydroperiod, variation from the mean and surface water extent of the wetlands, was found to be heavily influenced by short-term rainfall events observed in both abnormally wet and dry years, where staggered and persistent rainfall yielded the highest water surface area. Furthermore, the seasonal hydroperiod in many wetlands was found to be highly variable at sites when there is a decrease in either the temporary or semipermanent class. Temporary hydroperiod class was observed in higher ratios at times following extreme rain events compared with both seasonal and semipermanent.

Future research on the use of SAR for wetland hydroperiod classification would benefit from higher temporal resolution data to increase class reliability. The strength of the study is the ability to construct and examine meaningful hydroperiods of wetlands on large temporal and spatial scales that provide defining characteristics relevant to the current Alberta Environment and Sustainable Resource Development (ESRD) (2015) criteria, and better understanding the response of ungauged wetlands to precipitation events and evapotranspiration. This is of relevance to decision or policy makers requiring accurate and temporally representative analysis of wetlands being impacted by infrastructure, agriculture, or climate change. In addition, it will help hydrology models, as there is currently few prairie pothole wetland inventories. With the existing SAR satellites and inventory, such as RADARSAT-2, Sentinel, TerraSAR X, and the upcoming RCM, temporal resolution of many environmental monitoring processes involving the stacking of data can be greatly enhanced and applied to the hydroperiod methodology presented in this paper for monitoring wetlands.

The work presented is well suited to a systematic monitoring regime, as with the addition of new SAR data, the hydroperiod classification increases in accuracy and can be constantly updated, combining both monitoring and classification into a single framework. With

the fusion of optical and/or lidar data describing riparian vegetation communities, the hydroperiod analysis could be the basis for a more comprehensive wetland classification and monitoring framework. It also provides a valuable platform for land use permitting and regulation in heavily disturbed prairie or agri/urban landscapes, benefiting ecosystem service and function appreciations.

ACKNOWLEDGMENTS

The authors declare no conflict of interest. We acknowledge field assistance from Dr. Laura Chasmer, Mark Derksen, Ben Mindek, and Reed Parsons. RADARSAT-2 imagery was obtained and licensed from the Canada Centre for Mapping and Earth Observation, Earth Sciences Sector (Ottawa) and MDA with the assistance of Kevin Murnaghan (CCRS). Airborne LiDAR data (Airborne Imaging Inc., Calgary, AB) and RapidEye imagery (Planet., Lethbridge, AB) licensed to the Government of Alberta were used in the study. Hopkinson acknowledges funding for field and lab infrastructure from the Canada Foundation for Innovation and the Campus Alberta Innovates Program; project-related lab personnel, research and data funding to support SAR time-series wetland classification, and wetland ecosystem monitoring from Government of Alberta (Economic Development and Trade, Environment and Parks, and Agriculture and Forestry), Discovery Grant funding from the Natural Sciences and Engineering Research Council.

ORCID

Joshua S. Montgomery  <http://orcid.org/0000-0002-6220-2199>

Stewart B. Rood  <http://orcid.org/0000-0003-1340-1172>

REFERENCES

- Alberta Environment and Sustainable Resource Development (ESRD) (2015). *Alberta wetland classification system*. Edmonton, AB: Water Policy Branch, Policy and Planning Division.
- Ameli, A., & Creed, I. (2017). Quantifying hydrologic connectivity of wetlands to surface water systems. *Hydrology and Earth System Sciences*, 21(3), 1791–1808. <https://doi.org/10.5194/hess-21-1791-2017>
- Bolanos, S., Stiff, D., Brisco, B., & Pietroniro, A. (2016). Operational surface water detection and monitoring using Radarsat. *Remote Sensing*, 8, 285. <https://doi.org/10.3390/rs8040285>
- Brisco, B. (2015). Mapping and monitoring surface water and wetlands with synthetic aperture radar. In R. W. Tiner, M. W. Lang, & V. V. Klemas (Eds.), *Remote sensing of wetlands, applications and advances* (pp. 119–136). Boca Raton, Chapter 6: CRC Press.
- Brisco, B., Ahren, F., Murnaghan, K., White, L., Canisus, F., & Lancaster, P. (2017). Seasonal change in wetland coherence as an aid to wetland monitoring. *Remote Sensing*, 9, 158. <https://doi.org/10.3390/rs9020158>
- Burrough, P. A., Gaans, P. F. M., & MacMillan, R. A. (2000). High-resolution landform classification using fuzzy k-means. *Fuzzy Sets and Systems*, 113(1), 37–52. [https://doi.org/10.1016/S0165-0114\(99\)00011-1](https://doi.org/10.1016/S0165-0114(99)00011-1)
- Burrough, P. A., Wilson, J. P., & van Gaans, P. F. (2001). Fuzzy K-means classification of topo-climatic data as an aid to forest mapping in the Greater Yellowstone Area, USA. *Landscape Ecology*, 16, 523–546. <https://doi.org/10.1023/A:1013167712622>
- Canadian Space Agency (2016). RADARSAT Constellation. Available Online: <http://www.asc-csa.gc.ca/eng/satellites/radarsat>
- Cowardin, L. M., Carter, V., Golet, F. C., & LaRoe, E. T. (1979). Classification of Wetlands and Deepwater Habitats of the United States. FWS/OBS-79/31, 131p.

- Di Baldassarre, G., Shucmann, G., Brandimarte, L., & Bates, P. (2011). Timely low resolution SAR imagery to support floodplain modelings: A case study review. *Surveys in Geophysics*, 32, 255–269.
- Ewel, K. (1990). Swamps. In R. L. Myers, & J. J. Ewel (Eds.), *Ecosystems of Florida* (pp. 281–323). Orlando: University of Central Florida Press.
- Frey, K. E., & Smith, L. C. (2007). How well do we know northern land cover? Comparison of four global vegetation and wetland products with a new ground-truth database for West Siberia. *Global Biogeochemical Cycles*, 21, GB1016. <https://doi.org/10.1029/2006GB002706>
- Halsey, L. A., Vitt, D. H., Beilman, D., Crow, S., Mehelic, S., & Wells, R. (2004). *Alberta Wetland Inventory Classification System, version 2.0. Pub # T/031*. Edmonton, AB, Canada: Government of Alberta, Alberta Sustainable Resource Development.
- Hopkinson, C., Chasmer, L., Sass, G., Creed, I., Sitar, M., Kalbfleisch, W., & Treitz, P. (2005). Vegetation class dependent errors in lidar ground elevation and canopy height estimates in a boreal wetland environment. *Canadian Journal of Remote Sensing*, 31, 191–206.
- Irwin, K., Beaulne, D., Braun, A., & Fotopoulos, G. (2017). Fusion of SAR, optical and airborne lidar for surface water detection. *Remote Sensing*, 9, 890. <https://doi.org/10.3390/rs9090890>
- Kantrud, H. A., Millar, J. B., & Van Der Valk, A. G. (1989). *Northern prairie wetlands. Vegetation of wetlands of the prairie pothole region* (pp. 132–187). Ames, IA: Iowa State University Press.
- Kettridge, N., & Waddington, J. M. (2013). Towards quantifying the negative feedback regulation of peatland evaporation to drought. *Hydrological Processes*, 28, 11. <https://doi.org/10.1002/hyp.9898>
- Klein, E., Berg, E. E., & Dial, R. (2005). Wetland drying and succession across the Kenai Peninsula Lowlands, south-central Alaska. *Canadian Journal of Forest Research*, 35, 1931–1941.
- Lane, C. R., Liu, H., Autrey, B. C., Anenkhonov, O. A., Chepinoga, V., & Wu, Q. (2014). Improved wetland classification using eight-band high resolution satellite imagery and a hybrid approach. *Remote Sensing*, 6, 12187–12216. <https://doi.org/10.3390/rs61212187>
- Li, J., & Wang, S. (2017). Mapping water bodies using SAR imagery – an application over the Spiritwood valley aquifer, Manitoba. *Geomatics Canada, Open File 31*, 13. <https://doi.org/10.4095/300213>
- Lichvar, R. W., Melvin, N. C., Butterwick, M. L., & Kirchner, W. N. (2012). National wetland plant list indicator rating definitions. U.S. Army Corps of Engineers, Engineer Research and Development Center, Cold Regions Research and Engineering Laboratory ERDC/CRREL TR-12-1.
- Macdonald and Dettwiler and Associates Ltd (2016). Radarsat-2 product description. RN-SP-52-1238. Issue 1/13: March 21.
- Martinis, S., Kuenzer, C., Wendleder, A., & Dech, S. (2015). Comparing four operational SAR-based water and flood detection approaches. *International Journal of Remote Sensing*, 36(13), 3519–3543.
- McVicar, T. R., Roderick, M. L., Donohue, R. J., Li, L. T., Van Niel, T. G., Thomas, A., ... Dinpashoh, Y. (2012). Global review and synthesis of trends in observed terrestrial near-surface wind speeds: Implications for evaporation. *Journal of Hydrology*, 416–417, 182–205. <https://doi.org/10.1016/j.jhydrol.2011.10.024>
- Milly, P. C. D., & Dunne, K. A. (2011). On the hydrologic adjustment of climate-model projections: The potential pitfall of potential evapotranspiration. *Earth Interactions*, 15(1), 1–14. <https://doi.org/10.1175/2010EI363.1>
- Milly, P. C. D., & Dunne, K. A. (2016). Potential evapotranspiration and continental drying. *Nature Climate Change*, 6, 946–949. <https://doi.org/10.1038/nclimate304>
- Mitsch, W. J., & Gosselink, J. G. (2007). *Wetlands* (4th ed.). Hoboken, NJ: John Wiley & Sons, Inc.
- Natural Regions Committee (2006). Natural Regions and Subregions of Alberta. Compiled by D.J. Downing and W.W. Pettapiece. Government of Alberta. Pub No. T/852.
- Ozesmi, S. L., & Bauer, M. E. (2002). Satellite remote sensing of wetlands. *Wetlands Ecology and Management*, 10, 381–402.
- Peiman, R., Husam, A., Brisco, B., & Hopkinson, C. (2016). Performance evaluation of sar texture algorithms for surface water body extraction through an open source python-based engine. IGARSS.
- Riordan, B., Verbyla, D., & McGuire, A. D. (2006). Shrinking ponds in sub-arctic Alaska based on 1950–2002 remotely sensed images. *Journal of Geophysical Research*, 111, G04002.
- Roulet, N. T. (2000). Peatlands, carbon storage, greenhouse gases, and the Kyoto protocol, prospects and significance for Canada. *Wetlands*, 20, 605–615.
- Schlaffer, S., Chini, M., Dettmering, D., & Wagner, W. (2016). Mapping wetlands in Zambia using seasonal backscatter signatures derived from ENVISAT ASAR time series. *Remote Sensing*, 8(5), 402. <https://doi.org/10.3390/rs8050402>
- Schmitt, A., & Brisco, B. (2013). Wetland monitoring using the curvelet-based change detection method on polarimetric SAR imagery. *Water*, 5, 1036–1051.
- Schmitt, A., Liechtle, M., & Roth, H. (2012). On the use of dual-co-polarised terrasars-x data for wetland monitoring. *International Archives of the Photogrammetry, Remote Sensing and Spatial Information Sciences*, XXXIX-B7, 2012 XXII ISPRS Congress, 97–102.
- Stewart, R. E., & Kantrud, H. A. (1971). *Classification of natural ponds and lakes in the glaciated prairie region. Resource Publication 92* (p. 57). Washington, D.C.: Bureau of Sport Fisheries and Wildlife, U.S. Fish and Wildlife Service.
- Toutin, T. (2011). Corrigendum to the paper State-of-the-art of geometric correction of remote sensing data: a data fusion perspective. *International Journal of Image and Data Fusion*, 2, 283–286.
- Turetsky, M., Kane, E., Harden, J., Ottmar, R., Manies, K., Hoy, E., & Kasischke, E. (2011). Recent acceleration of biomass burning and carbon losses in Alaskan forests and peatlands. *Nature Geoscience*, 4(1), 21.
- White, L., Brisco, B., Daboor, M., Schmitt, A., & Pratt, A. (2015). A collection of SAR methodologies for monitoring wetlands. *Remote Sensing*, 7, 7615–7645. <https://doi.org/10.3390/rs70607615>
- White, L., Brisco, B., Pregitzer, M., Tedford, B., & Boychuck, L. (2014). RADARSAT-2 beam mode selection for surface water and flooded vegetation mapping. *Can. J. Remote Sensing*, 40, 135–151.
- Wild, M. (2009). Global dimming and brightening: A review. *Journal of Geophysical Research-Atmospheres*, 114, D00D16. <https://doi.org/10.1029/2008JD011470>
- Willett, K. M., Jones, P. D., Gillett, N. P., & Thorne, P. W. (2008). Recent changes in surface humidity: Development of the HadCRUH dataset. *Journal of Climate*, 21(20), 5364–5383.
- Winter, T. C. (1989). Hydrologic studies of wetlands in the northern prairie. In A. G. Van der valk (Ed.), *Northern prairie wetlands* (pp. 16–54). Ames: Iowa State University Press.
- Zhang, F., Xie, C., Li, K., Xu, M., Wang, X., & Xia, Z. (2012). Forest and deforestation identification based on multi-temporal polarimetric RADARSAT-2 images in Southwestern China. *Journal of Applied Remote Sensing*, 6, 063527. <https://doi.org/10.1117/1.JRS.6.063527>

How to cite this article: Montgomery JS, Hopkinson C, Brisco B, Patterson S, Rood SB. Wetland hydroperiod classification in the western prairies using multitemporal synthetic aperture radar. *Hydrological Processes*. 2018;32:1476–1490. <https://doi.org/10.1002/hyp.11506>